LAWRENCE LIVERMORE NATIONAL LABORATORY

LLNL-PROC-492563

Measurement Uncertainty of High Energy Density Science Target Assemblies for the National Ignition Facility

R. M. Seugling, W. W. Nederbragt, M. J. Wilson, K. J. M. Blobaum, S. C. Peterson, D. M. Lord

August 10, 2011

26th Annual Meeting of the American Society for Precision Engineering
Denver, CO, United States
November 13, 2011 through November 18, 2011

Measurement Uncertainty of High Energy Density Science Target Assemblies for the National Ignition Facility

Richard M. Seugling, Walter W. Nederbragt, Michael J. Wilson, Kerri J.M. Blobaum, Shawn C. Peterson, and Dawn M. Lord
Lawrence Livermore National Laboratory
Livermore, CA 94551

Introduction

Successful High Energy Density Science (HEDS) experiments at the National Ignition Facility (NIF) [1] require that millimeter-scale targets are fabricated, assembled, and measured with micrometer-scale tolerances. However, the materials and geometries involved in these assemblies present challenges for metrology and uncertainty quantification. The completed assemblies must accommodate both the features required for the physics experiment, as well as facility-dictated attributes such as shields, coatings and alignment fiducials. Here, we present an error analysis of target feature measurements, and propose solutions for minimizing uncertainty in future target designs.

Because of the fragility of the individual components and assemblies, optical metrology techniques [2] are used almost exclusively as a means of qualifying the final product. However, difficult-to-measure components such as dimpled metal shields, plastic coatings, and transparent features introduce uncertainties into these measurements and often require additional test procedures to determine the measurement uncertainty [3]. Furthermore, metrology of some individual components requires the use of alternate measurement techniques (e.g., contact probes). Combining these task-specific measurements [4] introduces additional uncertainties and has direct consequence to the success and/or failure of the experiment in terms of both interpreting the experimental results and properly aligning the target in the NIF target chamber.

Several different HEDS experiments are fielded on NIF, each requiring a different target configuration. The targets described here are all indirect drive experiments, where the laser beams are pointed into the laser entrance hole (LEH) of a gold hohlram aligned to the target chamber center (TCC). The 3Ω laser energy is converted into x-rays when the beams interact with the gold on the inside of the hohlraum. This

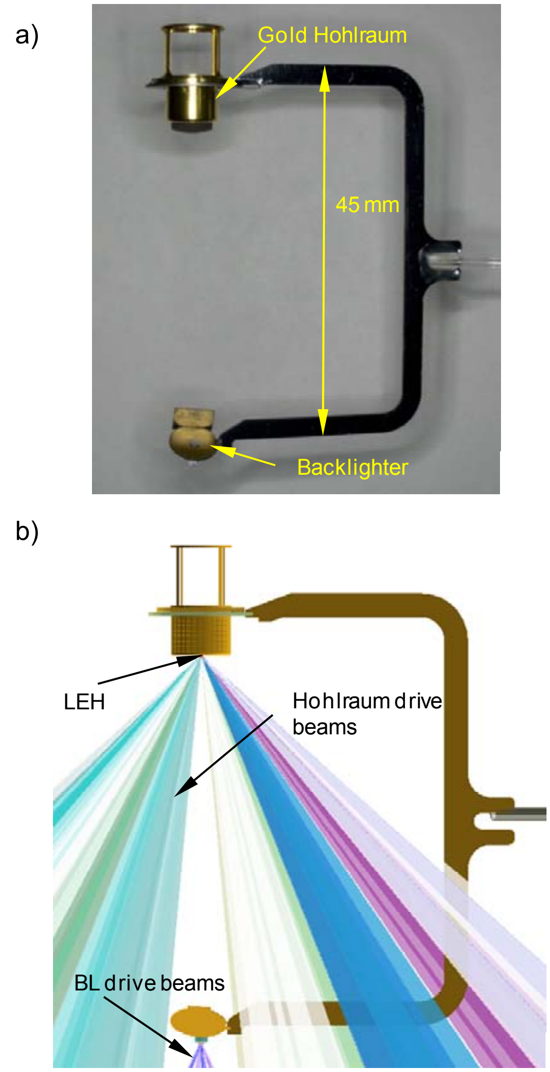

FIGURE 1. a) Photogragh of a streaked radiography target assembly. b) Model showing the laser drive beam entering the LEH and the backlighter drive beams hitting the microdot.

is the energy source for the experiment. Figure 1 illustrates one target configuration used to image x-ray flux through a low density material. The laser drive beams are pointed at a backlighter assembly (BL) directly below the LEH. The backlighter consists of a silver microdot on a Ta substrate with a laser machined slot that acts as the imaging x-ray source for the x-ray camera pointed at an aperture in the upper target assembly.

A schematic representation of the target/beam alignment is shown in Figure 2. The Target Alignment System (TAS) is located within the target chamber relative to the Chamber Coordinate Reference System (CCRS). Subsequently, the laser beams and Target Positioner (TARPOS) are aligned to the TAS. The positional accuracy required for a target relative to the TAS is ± 25 μm over the 5.0 m radius of the target chamber.

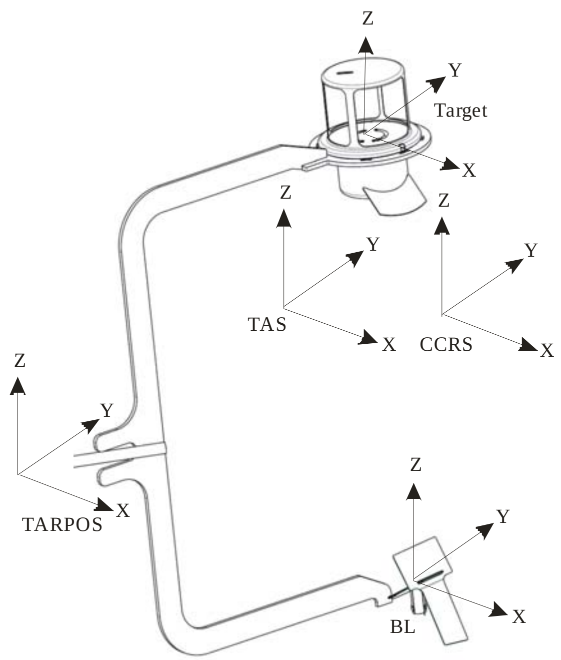

FIGURE 2. Illustration of the coordinate systems used for aligning a target within the NIF. Not shown are the additional coordinate systems representing diagnostic alignment.

In addition, various diagnostics are aligned to the target based on the location of TCC as determined by the TAS. The alignment accuracy of the diagnostics varies based on the type of system being used. For x-ray imaging systems, the allowable alignment error is on the order of ± 500 μm. For systems like the Velocity Interferometer System for Any Reflector (VISAR) used for measuring shock velocity, ± 100 μm can be required. The goal of this work is to quantify the uncertainty in the location of the target relative to TCC, based on measurement and alignment uncertainties.

Analysis

After target fabrication is complete, and before the target is transferred to the NIF target chamber, metrology of the target assembly is performed with optical coordinate measuring machines (OCMMs). To quantify the global effect of the task-specific measurement uncertainty, homogenous transformation matrices (HTMs) assuming small angles [6] were used to model the error sources and relate their influence to the overall target installation error budget. As is common in coordinate metrology, a local part or subassembly coordinate system (CS) is created. In the example shown in Figure 2, two separate coordinate systems will be defined for the target package and backlighter assembly.

A point derived from the OCMM is represented as follows

$$^{OCMM}\{P\} = \begin{Bmatrix} P_x + \delta x \\ P_y + \delta y \\ P_z + \delta z \end{Bmatrix}, \quad (1)$$

where P_x, P_y, and P_z are the X, Y, and Z coordinates and δx, δy, and δz are the measurement errors for each coordinate respectively. Each point is related to the part/subassembly CS expressed by

$$^{CS}\{P\}_{OCMM} = {}^{CS}[T]_{OCMM}\,{}^{OCMM}\{P\}, \quad (2)$$

where **T** is a transformation done by the OCMM. These points are used to create geometric features representing the measured assembly. These geometric features include the task specific measurement uncertainty which consist of errors associated with the machine, probe, algorithms, edge quality, the influence of coatings, etc.

Once each of the components and/or subassembly is defined by a set of points or geometric features the subassemblies are related to a common reference. For the case shown in Figure 2 the BL and TARPOS are defined relative to the target CS by

$$^{Tar}\{P\}_{BL} = {}^{Tar}[T]_{BL}\,{}^{BL}\{P\}, \quad (3)$$

$$^{Tar}\{P\}_{TPos} = {}^{Tar}[T]_{TPos}{}^{TPos}\{P\}. \quad (4)$$

Now the target is completely defined relative to the target CS. The final transformation relates the target assembly in the TARPOS to the TAS

$$^{TAS}\{P\}_{Tar} = {}^{TAS}[T]_{Tar}{}^{Tar}\{P\}, \quad (5)$$

where

$$^{Tar}\{P\} \quad = {}^{Tar}\{P\} + {}^{Tar}\{P\}_{BL} + {}^{Tar}\{P\}_{TPos}. \quad (6)$$

The error between the measured features and the TAS calculated by

$$^{TAS}\{E\} \quad = {}^{TAS}\{P\}_{Ideal} - {}^{TAS}\{P\}_{Measured}. \quad (7)$$

Removing second order terms, the error {E} for each coordinate is given by

$$\begin{aligned} ^{TAS}E_X \quad &= \varepsilon_{y,TAS}\left(\sum Z_{\text{offsets}}\right) - \varepsilon_{\text{y,TAS}}\left(\sum \text{Y}_{\text{offsets}}\right) \\ &+ \varepsilon_{\text{y,Tpos}}\left(P_{z,TPos}\right) + \varepsilon_{\text{y,BL}}\left(P_{z,BL}\right) - \varepsilon_{\text{z,TPos}}\left(P_{y,TPos}\right) \\ &- \varepsilon_{z,TPos}\left(P_{y,BL}\right) + \sum \delta_{x,comp}, \end{aligned} \quad (8)$$

$$\begin{aligned} ^{TAS}E_Y \quad &= \varepsilon_{z,TAS}\left(\sum X_{\text{offsets}}\right) - \varepsilon_{\text{x,TAS}}\left(\sum \text{Z}_{\text{offsets}}\right) \\ &+ \varepsilon_{\text{z,Tpos}}\left(P_{x,TPos}\right) + \varepsilon_{\text{z,BL}}\left(P_{x,BL}\right) - \varepsilon_{\text{x,TPos}}\left(P_{z,TPos}\right) \\ &- \varepsilon_{x,TPos}\left(P_{z,BL}\right) + \sum \delta_{y,comp}, \end{aligned} \quad (9)$$

$$\begin{aligned} ^{TAS}E_Z \quad &= \varepsilon_{x,TAS}\left(\sum Y_{\text{offsets}}\right) - \varepsilon_{\text{y,TAS}}\left(\sum \text{X}_{\text{offsets}}\right) \\ &+ \varepsilon_{\text{x,Tpos}}\left(P_{y,TPos}\right) + \varepsilon_{\text{x,BL}}\left(P_{y,BL}\right) - \varepsilon_{\text{y,TPos}}\left(P_{x,TPos}\right) \\ &- \varepsilon_{y,BL}\left(P_{y,BL}\right) + \sum \delta_{z,comp}, \end{aligned} \quad (10)$$

where X, Y and Z are relative offsets between features in the TAS CS, ε_x, ε_y and ε_z are the angular errors between CSs and δ_x, δ_y, and δ_z, are the displacement errors between CSs.

The analysis shown above represents key aspects of target manufacturing, with respect to metrology and system integration. The first two terms of eqs 8-10 represent the influence of the angular error and feature offsets between the target and the TAS within the NIF target chamber. In addition, the second set of terms in eqs 8-10 represent the tolerances required to define critical features, such as datums used to relate the BL and TARPOS to the target. This represents how well features need to be measured, but more importantly, how well datum features need to be defined. For the example shown in Figure 2 the calculated tolerance between the BL and Target and TARPOS and Target is on the order of 25 μm, which would ideally be verified by metrology having a measurement uncertainty of on the order of 2.5 μm.

Given these stringent requirements for alignment in the NIF chamber, it is necessary to integrate features specifically fabricated for this purpose into target designs. Depending on the type of experiment and drive configuration being utilized, there have been a number of different methods used to define alignment features. Figure 3 shows three different methods of transferring alignment information in the NIF target chamber. The target shown in a) has a 300 μm thick silicon washer as part of the target structure that acts as datum for both target metrology and alignment within the chamber. The Si washer has a total thickness variation of less than ± 1 μm and a flatness of better than ± 0.05 μm over the 9 mm diameter.

However, integrating a quality reference feature is not always applicable as illustrated by the examples shown in Figure 3 b) and c). In these cases, auxiliary parts such as dimpled aluminum shields used to reflect stray unconverted light from interfering with diagnostics impede measurement quality and often require additional features to be added specifically for chamber alignment. To transfer the datum information for alignment in the target chamber external fiducials have been added and measured on an OCMM to allow for insertion to a positional accuracy on the order of 25 μm.

Summary

Target alignment within the NIF chamber is a critical part of the overall success of an experimental campaign. Due to the stringent alignment requirements, target production including part/subassembly metrology and datum derivations needs to be considered throughout the design process. Typical measurement uncertainties for critical features is less than 10 μm, but can vary based on the overall target design and types of diagnostics being utilized during the experiment. In addition to alignment accuracy it is also important to have repeatable alignment procedures to expedite the shot cycle.

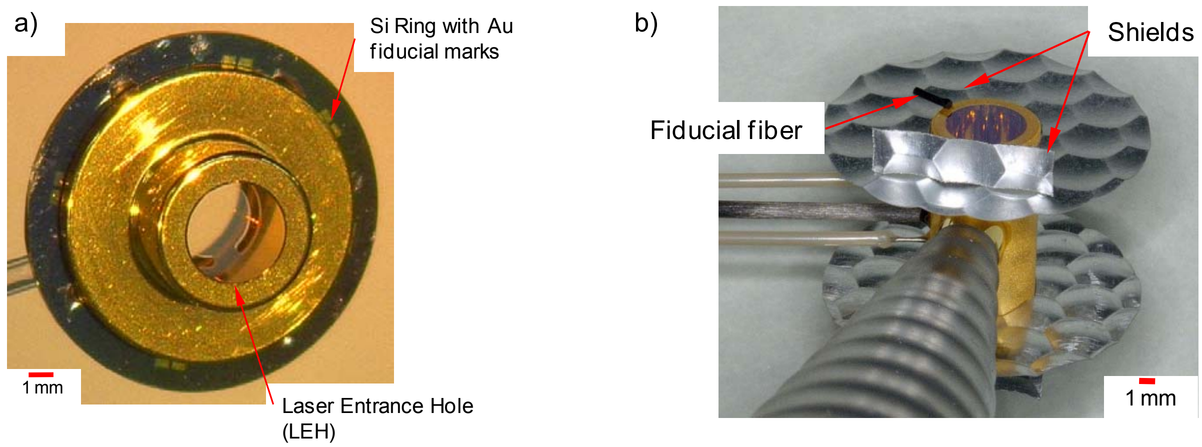

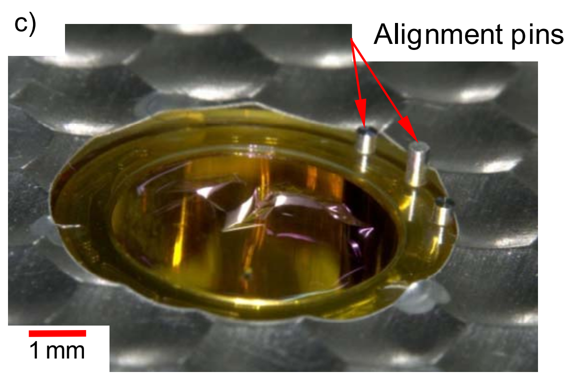

FIGURE 3. *a) HEDS single sided drive target configuration using Si ring with gold fiducial marks to create datum for both metrology and alignment in the NIF chamber. b) Equation-of-state target with alignment fiducial for setting Z location in the NIF target chamber. c) Alignment pins used to determine angular orientation and Z position within the target chamber.*

ACKNOWLEDGMENTS

The authors would like to thank the HEDS Manufacturing team – Dave Swift, Alex Hamza, Don Bennett, Pete DuPuy, Craig Akaba, Mike McClure, Steve Stodbecht, Rick Vargas, Gino Mercado, Kerry Bettencourt, Paul Mirkarimi, Joe Satcher, and John Sain from LLNL for their efforts in supporting this work.

This work was performed under the auspices of the U.S. Department of Energy by Lawrence Livermore National Laboratory under Contract DE-AC52-07NA27344.

References

[1] Moses, E., Overview of the National Ignition Facility, *Fusion Science and Technology*, 54 (**2**) 2008.
[2] Carmignato, S., Voltan, A. and Savio, E., Metrological performance of optical coordinate measuring machines under industrial conditions, *CIRP Annals*, 59 (**1**), 2010.
[3] Neuschaefer-Rube, U., Ehring, W., Neugebauer, M., and Wendt, K. Test procedures and artifacts for optical coordinate metrology, *Proc. of SPIE*, 1733, 2009.
[4] Wilhelm, W.G., Hocken, R. and Schwenke, H., Task Specific Uncertainty in Coordinate Measurement, *CIRP Annals*, 50 (**2**), 2001.
[5] Lindl, J.D., *Inertial Confinement Fusion: The Quest for Ignition and Energy Gain Using Indirect Drive*, Springer-Verlag, 1998.
[6] Slocum, A, *Precision Machine Design*, Prentice-Hall, 1992.